

EUROPEAN ORGANIZATION FOR NUCLEAR RESEARCH (CERN)



CERN-PH-EP-2014-297

LHCb-PAPER-2014-064

23 December 2014

Determination of the branching fractions of $B_s^0 \rightarrow D_s^\mp K^\pm$ and $B^0 \rightarrow D_s^- K^+$

The LHCb collaboration[†]

Abstract

Measurements are presented of the branching fractions of the decays $B_s^0 \rightarrow D_s^\mp K^\pm$ and $B^0 \rightarrow D_s^- K^+$ relative to the decays $B_s^0 \rightarrow D_s^- \pi^+$ and $B^0 \rightarrow D^- \pi^+$, respectively. The data used correspond to an integrated luminosity of 3.0 fb^{-1} of proton-proton collisions. The ratios of branching fractions are

$$\frac{\mathcal{B}(B_s^0 \rightarrow D_s^\mp K^\pm)}{\mathcal{B}(B_s^0 \rightarrow D_s^- \pi^+)} = 0.0752 \pm 0.0015 \pm 0.0019$$

and

$$\frac{\mathcal{B}(B^0 \rightarrow D_s^- K^+)}{\mathcal{B}(B^0 \rightarrow D^- \pi^+)} = 0.0129 \pm 0.0005 \pm 0.0008,$$

where the uncertainties are statistical and systematic, respectively.

Submitted to JHEP

© CERN on behalf of the LHCb collaboration, license CC-BY-4.0.

[†]Authors are listed at the end of this paper.

1 Introduction

The decays $B_s^0 \rightarrow D_s^\mp K^\pm$ offer a prime opportunity to measure CP violation in the interference between mixing and decay [1, 2]. The B_s^0 meson can decay into both charge-conjugate decays, providing sensitivity to the CKM angle γ [3]. The decays $B_s^0 \rightarrow D_s^\mp K^\pm$ and $B_s^0 \rightarrow D_s^- \pi^+$ occur predominantly through colour-allowed tree diagrams (see Fig. 1). A lower bound on the ratio of the $B_s^0 \rightarrow D_s^\mp K^\pm$ and $B_s^0 \rightarrow D_s^- \pi^+$ branching fractions was derived, $\mathcal{B}(B_s^0 \rightarrow D_s^\mp K^\pm)/\mathcal{B}(B_s^0 \rightarrow D_s^- \pi^+) \geq 0.080 \pm 0.007$ [4], with minimal external experimental and theoretical input. Using SU(3) flavour symmetry, and measurements of $B^0 \rightarrow D^- \pi^+$ decays at the B -factories, a prediction for the ratio of branching fractions was calculated, $\mathcal{B}(B_s^0 \rightarrow D_s^\mp K^\pm)/\mathcal{B}(B_s^0 \rightarrow D_s^- \pi^+) = 0.086^{+0.009}_{-0.007}$ [4], where the uncertainty includes contributions from non-factorisable effects [5] and from possible SU(3)-breaking effects of up to 20%. Contributions from the W -exchange diagram, absent in the decay $B_s^0 \rightarrow D_s^- \pi^+$, were estimated from the $B^0 \rightarrow D_s^- K^+$ branching fraction.

The CDF and Belle collaborations have pioneered the study of this ratio [6, 7], followed by the LHCb collaboration, which measured a ratio lower than the theoretical bound [8], using data corresponding to an integrated luminosity of 336 pb^{-1} . This paper presents an update for the absolute branching fraction of $B_s^0 \rightarrow D_s^\mp K^\pm$, and for the branching fraction of $B_s^0 \rightarrow D_s^\mp K^\pm$ relative to that of $B_s^0 \rightarrow D_s^- \pi^+$.

In addition, the ratio of branching fractions of the $B^0 \rightarrow D_s^- K^+$ and $B^0 \rightarrow D^- \pi^+$ decays is reported. The decay $B^0 \rightarrow D_s^- K^+$ proceeds through the colour-suppressed W -exchange

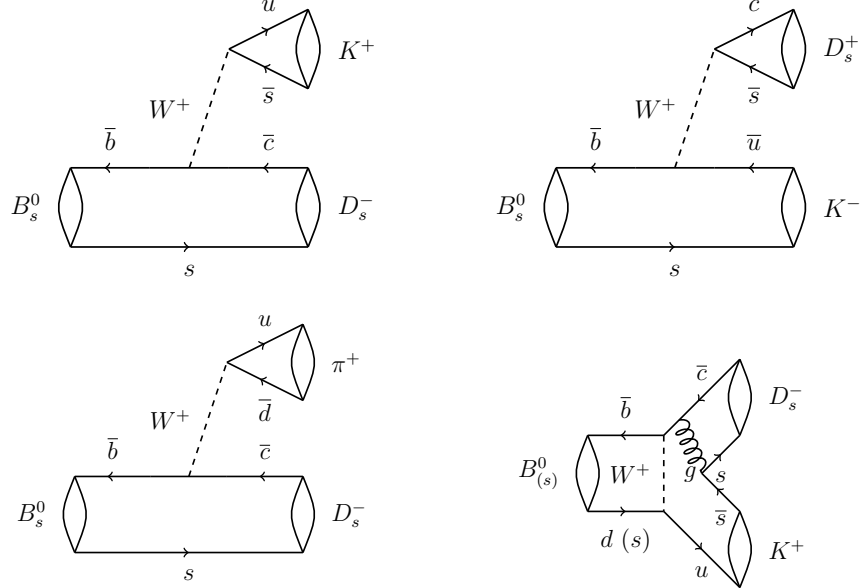


Figure 1: Feynman diagrams of the processes under study. The upper diagrams represent the two tree topologies in which a B_s^0 meson decays into the $D_s^\mp K^\pm$ final state, and the lower diagrams show the tree diagram of $B_s^0 \rightarrow D_s^- \pi^+$ and the W -exchange topology of $B_{(s)}^0 \rightarrow D_s^- K^+$.

diagram and the branching ratio determination allows the size of the W -exchange amplitude to be estimated, for example in the $B_s^0 \rightarrow D_s^\mp K^\pm$ decay. The existing branching fraction measurements by BaBar and Belle, $\mathcal{B}(B^0 \rightarrow D_s^- K^+) = (2.9 \pm 0.4 \text{ (stat)} \pm 0.2 \text{ (syst)}) \times 10^{-5}$ [9] and $(1.91 \pm 0.24 \text{ (stat)} \pm 0.17 \text{ (syst)}) \times 10^{-5}$ [10], respectively, show a difference of about 1.8 standard deviations, and suggest that an enhancement of the branching fraction due to rescattering effects is small [11]. Note that throughout this paper, charge conjugation is implied, and thus that the branching fraction $\mathcal{B}(B_{(s)}^0)$ corresponds to the average of the branching fraction of the $B_{(s)}^0$ decay and the $\bar{B}_{(s)}^0$ decay.

The pp -collision data used in this analysis correspond to an integrated luminosity of 3.0 fb^{-1} , of which 1.0 fb^{-1} was collected by LHCb in 2011 at a centre-of-mass energy of $\sqrt{s} = 7 \text{ TeV}$, and the remaining 2.0 fb^{-1} in 2012 at $\sqrt{s} = 8 \text{ TeV}$.

The LHCb detector [12] is a single-arm forward spectrometer covering the pseudorapidity range $2 < \eta < 5$, designed for the study of particles containing b or c quarks. The detector includes a high-precision tracking system consisting of a silicon-strip vertex detector surrounding the pp interaction region, a large-area silicon-strip detector located upstream of a dipole magnet with a bending power of about 4 Tm, and three stations of silicon-strip detectors and straw drift tubes placed downstream of the magnet. The polarity of the magnet is reversed periodically throughout data-taking. The tracking system provides a measurement of momentum, p , with a relative uncertainty that varies from 0.4% at low momentum to 0.6% at $100 \text{ GeV}/c$. The minimum distance of a track to a primary vertex, the impact parameter, is measured with a resolution of $(15 + 29/p_T) \mu\text{m}$, where p_T is the component of p transverse to the beam, in GeV/c . Different types of charged hadrons are distinguished using information from two ring-imaging detectors.

The trigger consists of a hardware stage, based on information from the calorimeter and muon systems, followed by a software stage, which applies a full event reconstruction. The software trigger requires a two-, three- or four-track secondary vertex with a significant displacement from the primary pp interaction vertices (PVs). At least one charged particle must have a transverse momentum $p_T > 1.7 \text{ GeV}/c$ and be inconsistent with originating from the PV. A multivariate algorithm [13] is used for the identification of secondary vertices consistent with the decay of a b hadron.

In the simulation, pp collisions are generated using PYTHIA [14] with a specific LHCb configuration [15]. Decays of hadronic particles are described by EVTGEN [16]. The interaction of the generated particles with the detector and its response are implemented using the GEANT4 toolkit [17] as described in Ref. [18].

2 Event selection

Candidate $B_{(s)}^0$ mesons are reconstructed by combining a $D_{(s)}^\pm$ candidate decaying into three light hadrons, $D^- \rightarrow K^+ \pi^- \pi^-$ or $D_s^- \rightarrow K^+ K^- \pi^-$, with an additional pion or kaon (the “bachelor” particle). Each of the four final-state light hadrons is required to have a good track quality, high momentum and transverse momentum, and a large impact parameter with respect to the primary vertex. The contribution from charmless

Table 1: Kinematic and PID selection efficiencies for each signal decay, as determined from simulated events and data, respectively. The kinematic efficiencies represent weighted averages determined from events simulated at $\sqrt{s} = 7$ TeV (34%) and $\sqrt{s} = 8$ TeV (66%). The binomial uncertainties result from the size of the simulated samples.

Selection efficiency (%)	Kinematic	PID	Total
$B^0 \rightarrow D^- \pi^+$	1.89 ± 0.01	74.29 ± 0.07	1.40 ± 0.01
$B_s^0 \rightarrow D_s^- \pi^+$	1.92 ± 0.02	67.10 ± 0.09	1.29 ± 0.01
$B_s^0 \rightarrow D_s^\mp K^\pm$	2.08 ± 0.01	55.52 ± 0.17	1.15 ± 0.01
$B^0 \rightarrow D_s^- K^+$	1.70 ± 0.03	58.11 ± 0.82	0.99 ± 0.02

$B_{(s)}^0$ decays, such as $B_s^0 \rightarrow K^+ K^- \pi^+ \pi^-$, is suppressed by requiring the $D_{(s)}^\pm$ candidate to have a significant flight distance from the reconstructed $B_{(s)}^0$ decay vertex, and by requiring its mass to fall within a small mass window of $^{+22}_{-24}$ MeV/ c^2 around the $D_{(s)}^\pm$ mass [19]. To reduce the combinatorial background, a multivariate algorithm is applied. This boosted decision tree (BDT) [20, 21] is identical to that used in the analysis of the CP asymmetry in $B_s^0 \rightarrow D_s^\mp K^\pm$ decays [3], and was trained with $B_s^0 \rightarrow D_s^- \pi^+$ candidates from data, using a weighted data sample based on the *sPlot* technique [22] as signal and candidates with an invariant mass greater than 5445 MeV/ c^2 as background. The variables with the highest discriminating power are found to be the difference between the χ^2 from the vertex fit of the associated PV reconstructed with and without the considered b -hadron candidate, the p_T of the final-state particles, and the angle between the b -hadron momentum vector and the vector connecting its production and decay vertices.

Misidentification of particles leads to peaking backgrounds in the signal region, for example $B_s^0 \rightarrow D_s^- \pi^+$ events reconstructed as $B_s^0 \rightarrow D_s^\mp K^\pm$ candidates. Pions and kaons in these decays are required to satisfy particle identification (PID) requirements, and approximately 60% of the signal is retained while over 99% of the background is rejected. The efficiencies of these requirements are determined by studying kinematically selected $D^{*+} \rightarrow D^0 (\rightarrow K^- \pi^+) \pi^+$ and $\Lambda \rightarrow p \pi^-$ decays obtained from data, which provide high-purity PID.

In the $B^0 \rightarrow D^- \pi^+$ selection, loose PID requirements are applied since the branching fraction of the signal process is much larger than those of background decays resulting from misidentification. In the $B_s^0 \rightarrow D_s^- \pi^+$ and $B_s^0 \rightarrow D_s^\mp K^\pm$ selections, a stricter requirement is applied to the D_s^+ decays to distinguish D_s^+ and D^+ mesons. For these decays, a further selection requirement is applied to reduce the background from $\Lambda_b^0 \rightarrow \Lambda_c^+ \pi^-$ decays, where one of the D_s^+ daughters is misidentified as a proton. This requirement removes any candidate which fulfils two criteria: that there is a large probability for one of the D_s^+ daughters to be a misidentified proton, and that when the D_s^+ decay is reconstructed under the Λ_c^+ hypothesis, its invariant mass falls within 21 MeV/ c^2 of the nominal Λ_c^+ mass [19]. This procedure almost fully eliminates this background. The

efficiency of the selection is obtained from simulation and is summarised in Table 1.

3 Signal yield determination

An unbinned maximum likelihood fit to the candidate invariant mass distribution is performed for each of the three final states. The signal shapes are parametrised by a double-sided Crystal Ball shape [23]. This function consists of a central Gaussian part, whose mean and width are free parameters, and power-law tails on both lower and upper sides, to account for energy loss due to final-state radiation and detector resolution effects. The functional form for the combinatorial background, an exponential function with an offset, is obtained from same-charge $D_s^\pm\pi^\pm$ combinations. All parameters of the combinatorial background are left free in the fit to data.

The physical backgrounds can be split into two categories: misidentified backgrounds, predominantly where one of the final state pions (kaons) is mistaken for a kaon (pion); and partially reconstructed backgrounds, where a neutral pion or a photon is not included in the candidate reconstruction, causing the reconstructed $B_{(s)}^0$ mass to shift to lower values. Some backgrounds fall into both categories. The number of background components considered varies per final state. The invariant mass shapes of these backgrounds are obtained from simulation at $\sqrt{s} = 8$ TeV, with the event selection applied. The yield of each background is a parameter in the fit, with most background components Gaussian-constrained around the expected yield normalised to the $B^0 \rightarrow D^- \pi^+$ yield obtained from data. The constraints are assigned an uncertainty of 10%, which reflects the uncertainties from production fractions, branching fractions, and reconstruction efficiencies. The resulting background yields from the fit are close to the expected values. The results of the fits for the three final states are shown in Figs. 2 and 3, and in Table 2. The three fits are independent, and no parameters are shared among them.

Various consistency checks are performed for each of the fits. The fitted yield of $B_s^0 \rightarrow D_s^- \pi^+$ events reconstructed in the $D_s^\mp K^\pm$ final state, which is allowed to vary in the fit, is consistent with the expected yield based on the relative branching fraction, particle misidentification probability and reconstruction efficiency. For each of the fits, consistency is also found between the fitted yield for both magnet polarities separately and the fraction of data corresponding to that polarity. This demonstrates that the relative yields are

Table 2: Yields for the four signal decay types, as obtained from the fits.

	Yield
$B^0 \rightarrow D^- \pi^+$	$458\,940 \pm 959$
$B_s^0 \rightarrow D_s^- \pi^+$	$75\,566 \pm 342$
$B_s^0 \rightarrow D_s^\mp K^\pm$	$5\,101 \pm 100$
$B^0 \rightarrow D_s^- K^+$	$2\,452 \pm 98$

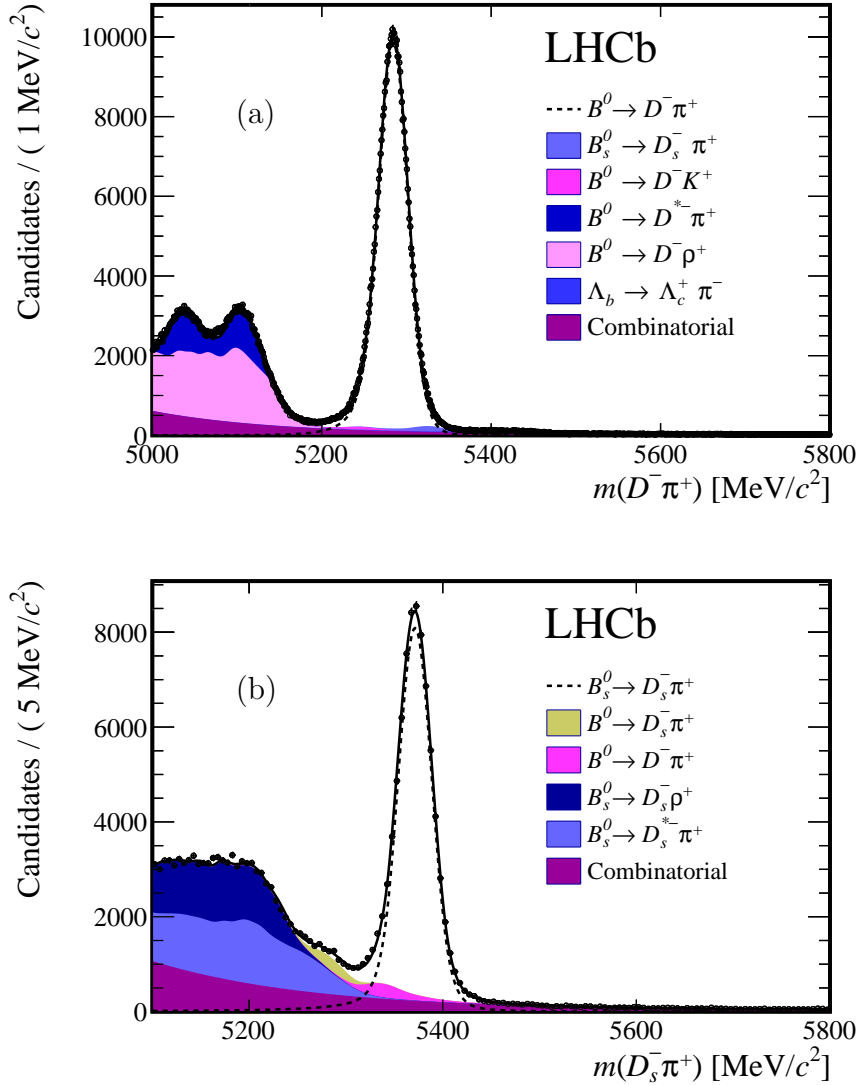


Figure 2: Results of the fits to the invariant mass distributions of the final states (a) $D^- \pi^+$ and (b) $D_s^- \pi^+$.

stable as a function of time and magnet polarity.

4 Systematic uncertainties

Systematic uncertainties arise from the fit model and the candidate selection, and are summarised in Table 3. The systematic uncertainty from the fit model is determined by applying variations to the fit model and comparing the yield to the nominal result,

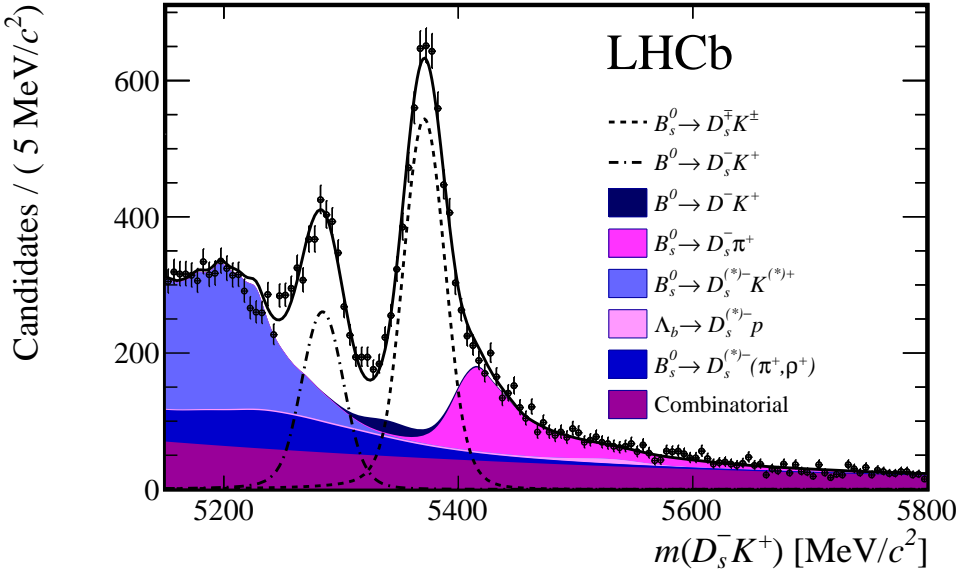


Figure 3: Result of the fit to the invariant mass distribution of the final state $D_s^{\mp}K^{\pm}$.

taking the difference as a systematic uncertainty. These variations include a different combinatorial shape, fixing the signal shape tail parameters to values obtained from simulation, and using background shapes determined from simulation matching the LHCb conditions during 2011 ($\sqrt{s} = 7$ TeV). In the $D^- \pi^+$ analysis, the fit range is reduced to start at 5100 MeV/ c^2 . In the $D_s^{\mp}K^{\pm}$ analysis, the as yet unobserved decay $\Lambda_b^0 \rightarrow D_s^- p$ is omitted from the fit.

The uncertainty on the candidate selection is separated into three parts: the uncertainty due to the differences between data and simulation, that due to the PID requirements on the final state pions and kaons, and that due to the hardware trigger efficiency. The first of these uncertainties is determined from the selection efficiency difference between magnet polarities in simulation, and by estimating the uncertainty on the BDT selection efficiency due to differences between data and simulation. This is calculated by reweighting simulated events to match the data more closely, and calculating the difference in BDT efficiency between those and the unweighted samples. The uncertainty on the PID efficiency and misidentification rate is estimated by comparing the PID performance measured using a simulated D^* calibration sample with that observed in simulated signal events. The systematic uncertainty from the hardware trigger efficiency arises from differences in the pion and kaon trigger efficiencies which are not reproduced in the simulation. The uncertainty is scaled with the fraction of events where a signal track was responsible for triggering.

A further systematic uncertainty is added to account for possible charmless B^0 decays peaking under the $B^0 \rightarrow D_s^- K^+$ signal. Some of the uncertainties cancel in the ratios of

Table 3: Systematic uncertainties on the ratios of branching fractions, in %, obtained as described in the text. The total uncertainty is obtained by adding the separate contributions in quadrature.

Source	$\frac{B_s^0 \rightarrow D_s^\mp K^\pm}{B_s^0 \rightarrow D_s^- \pi^+}$	$\frac{B^0 \rightarrow D_s^- K^+}{B^0 \rightarrow D^- \pi^+}$
	$B_s^0 \rightarrow D_s^\mp K^\pm$	$B^0 \rightarrow D_s^- K^+$
Fit model	1.1	3.6
Candidate selection	2.1	2.9
Hardware trigger	1.0	1.2
Charmless background	–	1.0
Total	2.5	4.9

branching fractions, leading to lower overall systematic uncertainties than those determined individually for each decay channel.

5 Determination of branching fractions

The ratios of branching fractions are evaluated using the expression

$$\frac{\mathcal{B}(A)}{\mathcal{B}(B)} = \frac{\varepsilon_B N_A f_B}{\varepsilon_A N_B f_A} \frac{\mathcal{B}_{D_{(s)}^\pm}}{\mathcal{B}_{D_{(s)}^\pm}}, \quad (1)$$

where ε_X , f_X and N_X are the selection efficiency, the hadronisation fraction, and the fitted yield of decay X , respectively, and $\mathcal{B}_{D_{(s)}^\pm}$ is the branching fraction of $D_{(s)}^\pm$ decays, as appropriate. The following values are used as input [19]:

$$\begin{aligned} \mathcal{B}(B^0 \rightarrow D^- \pi^+) &= (2.68 \pm 0.13) \times 10^{-3}, \\ \mathcal{B}(B_s^0 \rightarrow D_s^- \pi^+) &= (3.04 \pm 0.23) \times 10^{-3}, \\ \mathcal{B}(D^- \rightarrow K^+ \pi^- \pi^-) &= (9.13 \pm 0.19) \times 10^{-2}, \\ \mathcal{B}(D_s^- \rightarrow K^+ K^- \pi^-) &= (5.39 \pm 0.21) \times 10^{-2}. \end{aligned}$$

As a cross-check, a value $\mathcal{B}(B_s^0 \rightarrow D_s^- \pi^+) = (2.95 \pm 0.01 \text{ (stat)}) \times 10^{-3}$ was obtained from the measured $B_s^0 \rightarrow D_s^- \pi^+$ and $B^0 \rightarrow D^- \pi^+$ yields using Eq. (1). This measurement is compatible with the world-average value, and the central value is unchanged with respect to the previous result published by LHCb [8].

The following results are obtained

$$\begin{aligned}\frac{\mathcal{B}(B_s^0 \rightarrow D_s^\mp K^\pm)}{\mathcal{B}(B_s^0 \rightarrow D_s^- \pi^+)} &= 0.0752 \pm 0.0015 \text{ (stat)} \pm 0.0019 \text{ (syst)}, \\ \mathcal{B}(B_s^0 \rightarrow D_s^\mp K^\pm) &= (2.29 \pm 0.05 \text{ (stat)} \pm 0.06 \text{ (syst)} \pm 0.17(\mathcal{B}_{B_s^0})) \times 10^{-4}, \\ \frac{\mathcal{B}(B^0 \rightarrow D_s^- K^+)}{\mathcal{B}(B^0 \rightarrow D^- \pi^+)} &= 0.0129 \pm 0.0005 \text{ (stat)} \pm 0.0007 \text{ (syst)} \pm 0.0004(\mathcal{B}_{D_{(s)}^\pm}), \\ \mathcal{B}(B^0 \rightarrow D_s^- K^+) &= (3.45 \pm 0.14 \text{ (stat)} \pm 0.20 \text{ (syst)} \pm 0.20(\mathcal{B}_{B^0, D_{(s)}^\pm})) \times 10^{-5},\end{aligned}$$

where the uncertainties labelled (\mathcal{B}) arise from the uncertainties on the branching fractions used as input.

The branching fractions of $B_s^0 \rightarrow D_s^\mp K^\pm$ and $B^0 \rightarrow D_s^- K^+$ presented here are more precise than the current world-average values. The result for $\mathcal{B}(B_s^0 \rightarrow D_s^\mp K^\pm)/\mathcal{B}(B_s^0 \rightarrow D_s^- \pi^+)$ is compatible with theoretical expectations [4]. As expected [5], the branching fraction of the decay $B^0 \rightarrow D_s^- K^+$, dominated by the W -exchange topology, is suppressed compared to the decay $B^0 \rightarrow D^- \pi^+$, which predominantly proceeds through the colour-allowed tree topology. The measured value of $\mathcal{B}(B^0 \rightarrow D_s^- K^+)$ is in good agreement with existing measurements from the BaBar collaboration [9], and is larger than the result published by the Belle collaboration [10] with a significance of more than three standard deviations.

Acknowledgements

We express our gratitude to our colleagues in the CERN accelerator departments for the excellent performance of the LHC. We thank the technical and administrative staff at the LHCb institutes. We acknowledge support from CERN and from the national agencies: CAPES, CNPq, FAPERJ and FINEP (Brazil); NSFC (China); CNRS/IN2P3 (France); BMBF, DFG, HGF and MPG (Germany); INFN (Italy); FOM and NWO (The Netherlands); MNiSW and NCN (Poland); MEN/IFA (Romania); MinES and FANO (Russia); MinECo (Spain); SNSF and SER (Switzerland); NASU (Ukraine); STFC (United Kingdom); NSF (USA). The Tier1 computing centres are supported by IN2P3 (France), KIT and BMBF (Germany), INFN (Italy), NWO and SURF (The Netherlands), PIC (Spain), GridPP (United Kingdom). We are indebted to the communities behind the multiple open source software packages on which we depend. We are also thankful for the computing resources and the access to software R&D tools provided by Yandex LLC (Russia). Individual groups or members have received support from EPLANET, Marie Skłodowska-Curie Actions and ERC (European Union), Conseil général de Haute-Savoie, Labex ENIGMASS and OCEVU, Région Auvergne (France), RFBR (Russia), XuntaGal and GENCAT (Spain), Royal Society and Royal Commission for the Exhibition of 1851 (United Kingdom).

References

- [1] R. Aleksan, I. Dunietz, and B. Kayser, *Determining the CP-violating phase γ* , Z. Phys. **C54** (1992) 653.
- [2] R. Fleischer, *New strategies to obtain insights into CP violation through $B_s \rightarrow D_s^\pm K^\mp, D_s^{*\pm} K^\mp, \dots$ and $B_d \rightarrow D^\pm \pi^\mp, D^{*\pm} \pi^\mp, \dots$ decays*, Nucl. Phys. **B671** (2003) 459, [arXiv:hep-ph/0304027](#).
- [3] LHCb collaboration, R. Aaij *et al.*, *Measurement of CP asymmetry in $B_s^0 \rightarrow D_s^\mp K^\pm$ decays*, JHEP **11** (2014) 060, [arXiv:1407.6127](#).
- [4] K. De Bruyn *et al.*, *Exploring $B_s \rightarrow D_s^{(*)\pm} K^\mp$ decays in the presence of a sizable width difference $\Delta\Gamma_s$* , Nucl. Phys. **B868** (2012) 351, [arXiv:1208.6463](#).
- [5] R. Fleischer, N. Serra, and N. Tuning, *Tests of factorization and SU(3) relations in B decays into heavy-light final states*, Phys. Rev. **D83** (2011) 014017, [arXiv:1012.2784](#).
- [6] CDF collaboration, T. Aaltonen *et al.*, *First observation of $\bar{B}_s^0 \rightarrow D_s^\pm K^\mp$ and measurement of the ratio of branching fractions $B(\bar{B}_s^0 \rightarrow D_s^\pm K^\mp) / B(\bar{B}_s^0 \rightarrow D_s^+ \pi^-)$* , Phys. Rev. Lett. **103** (2009) 191802, [arXiv:0809.0080](#).
- [7] Belle collaboration, R. Louvot *et al.*, *Measurement of the decay $B_s^0 \rightarrow D_s^- \pi^+$ and evidence for $B_s^0 \rightarrow D_s^\pm K^\pm$ in e^+e^- annihilation at $\sqrt{s} \sim 10.87$ GeV*, Phys. Rev. Lett. **102** (2009) 021801, [arXiv:0809.2526](#).
- [8] LHCb collaboration, R. Aaij *et al.*, *Measurements of the branching fractions of the decays $B_s^0 \rightarrow D_s^\mp K^\pm$ and $B_s^0 \rightarrow D_s^- \pi^+$* , JHEP **06** (2012) 115, [arXiv:1204.1237](#).
- [9] BaBar collaboration, B. Aubert *et al.*, *Measurement of the branching fractions of the rare decays $B^0 \rightarrow D_s^{(*)+} \pi^-$, $B^0 \rightarrow D_s^{(*)+} \rho^-$, and $B^0 \rightarrow D_s^{(*)-} K^{(*)+}$* , Phys. Rev. **D78** (2008) 032005, [arXiv:0803.4296](#).
- [10] Belle collaboration, A. Das *et al.*, *Measurements of branching fractions for $B^0 \rightarrow D_s^+ \pi^-$ and $\bar{B}^0 \rightarrow D_s^+ K^-$* , Phys. Rev. **D82** (2010) 051103, [arXiv:1007.4619](#).
- [11] M. Gronau and J. L. Rosner, *B decays dominated by $\omega - \phi$ mixing*, Phys. Lett. **B666** (2008) 185, [arXiv:0806.3584](#).
- [12] LHCb collaboration, A. A. Alves Jr. *et al.*, *The LHCb detector at the LHC*, JINST **3** (2008) S08005.
- [13] V. V. Gligorov and M. Williams, *Efficient, reliable and fast high-level triggering using a bonsai boosted decision tree*, JINST **8** (2013) P02013, [arXiv:1210.6861](#).

- [14] T. Sjöstrand, S. Mrenna, and P. Skands, *PYTHIA 6.4 physics and manual*, JHEP **05** (2006) 026, [arXiv:hep-ph/0603175](#); T. Sjöstrand, S. Mrenna, and P. Skands, *A brief introduction to PYTHIA 8.1*, Comput. Phys. Commun. **178** (2008) 852, [arXiv:0710.3820](#).
- [15] I. Belyaev *et al.*, *Handling of the generation of primary events in Gauss, the LHCb simulation framework*, Nuclear Science Symposium Conference Record (NSS/MIC) **IEEE** (2010) 1155.
- [16] D. J. Lange, *The EvtGen particle decay simulation package*, Nucl. Instrum. Meth. **A462** (2001) 152.
- [17] Geant4 collaboration, J. Allison *et al.*, *Geant4 developments and applications*, IEEE Trans. Nucl. Sci. **53** (2006) 270; Geant4 collaboration, S. Agostinelli *et al.*, *Geant4: a simulation toolkit*, Nucl. Instrum. Meth. **A506** (2003) 250.
- [18] M. Clemencic *et al.*, *The LHCb simulation application, Gauss: Design, evolution and experience*, J. Phys. Conf. Ser. **331** (2011) 032023.
- [19] Particle Data Group, K. A. Olive *et al.*, *Review of particle physics*, Chin. Phys. **C38** (2014) 090001.
- [20] L. Breiman, J. H. Friedman, R. A. Olshen, and C. J. Stone, *Classification and regression trees*, Wadsworth international group, Belmont, California, USA, 1984.
- [21] R. E. Schapire and Y. Freund, *A decision-theoretic generalization of on-line learning and an application to boosting*, Jour. Comp. and Syst. Sc. **55** (1997) 119.
- [22] M. Pivk and F. R. Le Diberder, *sPlot: A statistical tool to unfold data distributions*, Nucl. Instrum. Meth. **A555** (2005) 356, [arXiv:physics/0402083](#).
- [23] T. Skwarnicki, *A study of the radiative cascade transitions between the Upsilon-prime and Upsilon resonances*, PhD thesis, Institute of Nuclear Physics, Krakow, 1986, DESY-F31-86-02.

LHCb collaboration

R. Aaij⁴¹, B. Adeva³⁷, M. Adinolfi⁴⁶, A. Affolder⁵², Z. Ajaltouni⁵, S. Akar⁶, J. Albrecht⁹, F. Alessio³⁸, M. Alexander⁵¹, S. Ali⁴¹, G. Alkhazov³⁰, P. Alvarez Cartelle³⁷, A.A. Alves Jr^{25,38}, S. Amato², S. Amerio²², Y. Amhis⁷, L. An³, L. Anderlini^{17,g}, J. Anderson⁴⁰, R. Andreassen⁵⁷, M. Andreotti^{16,f}, J.E. Andrews⁵⁸, R.B. Appleby⁵⁴, O. Aquines Gutierrez¹⁰, F. Archilli³⁸, A. Artamonov³⁵, M. Artuso⁵⁹, E. Aslanides⁶, G. Auriemma^{25,n}, M. Baalouch⁵, S. Bachmann¹¹, J.J. Back⁴⁸, A. Badalov³⁶, C. Baesso⁶⁰, W. Baldini¹⁶, R.J. Barlow⁵⁴, C. Barschel³⁸, S. Barsuk⁷, W. Barter⁴⁷, V. Batozskaya²⁸, V. Battista³⁹, A. Bay³⁹, L. Beaucourt⁴, J. Beddow⁵¹, F. Bedeschi²³, I. Bediaga¹, L.J. Bel⁴¹, S. Belogurov³¹, K. Belous³⁵, I. Belyaev³¹, E. Ben-Haim⁸, G. Bencivenni¹⁸, S. Benson³⁸, J. Benton⁴⁶, A. Berezhnoy³², R. Bernet⁴⁰, A. Bertolin²², M.-O. Bettler⁴⁷, M. van Beuzekom⁴¹, A. Bien¹¹, S. Bifani⁴⁵, T. Bird⁵⁴, A. Bizzeti^{17,i}, P.M. Bjørnstad⁵⁴, T. Blake⁴⁸, F. Blanc³⁹, J. Blouw¹⁰, S. Blusk⁵⁹, V. Bocci²⁵, A. Bondar³⁴, N. Bondar^{30,38}, W. Bonivento¹⁵, S. Borghi⁵⁴, A. Borgia⁵⁹, M. Borsato⁷, T.J.V. Bowcock⁵², E. Bowen⁴⁰, C. Bozzi¹⁶, D. Brett⁵⁴, M. Britsch¹⁰, T. Britton⁵⁹, J. Brodzicka⁵⁴, N.H. Brook⁴⁶, A. Bursche⁴⁰, J. Buytaert³⁸, S. Cadeddu¹⁵, R. Calabrese^{16,f}, M. Calvi^{20,k}, M. Calvo Gomez^{36,p}, P. Campana¹⁸, D. Campora Perez³⁸, L. Capriotti⁵⁴, A. Carbone^{14,d}, G. Carboni^{24,l}, R. Cardinale^{19,38,j}, A. Cardini¹⁵, L. Carson⁵⁰, K. Carvalho Akiba^{2,38}, RCM Casanova Mohr³⁶, G. Cassé⁵², L. Cassina^{20,k}, L. Castillo Garcia³⁸, M. Cattaneo³⁸, Ch. Cauet⁹, R. Cenci^{23,t}, M. Charles⁸, Ph. Charpentier³⁸, M. Chefdeville⁴, S. Chen⁵⁴, S.-F. Cheung⁵⁵, N. Chiapolini⁴⁰, M. Chrzaszcz^{40,26}, X. Cid Vidal³⁸, G. Ciezarek⁴¹, P.E.L. Clarke⁵⁰, M. Clemencic³⁸, H.V. Cliff⁴⁷, J. Closier³⁸, V. Coco³⁸, J. Cogan⁶, E. Cogneras⁵, V. Cogoni¹⁵, L. Cojocariu²⁹, G. Collazuol²², P. Collins³⁸, A. Comerma-Montells¹¹, A. Contu^{15,38}, A. Cook⁴⁶, M. Coombes⁴⁶, S. Coquereau⁸, G. Corti³⁸, M. Corvo^{16,f}, I. Counts⁵⁶, B. Couturier³⁸, G.A. Cowan⁵⁰, D.C. Craik⁴⁸, A.C. Crocombe⁴⁸, M. Cruz Torres⁶⁰, S. Cunliffe⁵³, R. Currie⁵³, C. D'Ambrosio³⁸, J. Dalseno⁴⁶, P. David⁸, P.N.Y. David⁴¹, A. Davis⁵⁷, K. De Bruyn⁴¹, S. De Capua⁵⁴, M. De Cian¹¹, J.M. De Miranda¹, L. De Paula², W. De Silva⁵⁷, P. De Simone¹⁸, C.-T. Dean⁵¹, D. Decamp⁴, M. Deckenhoff⁹, L. Del Buono⁸, N. Déléage⁴, D. Derkach⁵⁵, O. Deschamps⁵, F. Dettori³⁸, B. Dey⁴⁰, A. Di Canto³⁸, A Di Domenico²⁵, F. Di Ruscio²⁴, H. Dijkstra³⁸, S. Donleavy⁵², F. Dordei¹¹, M. Dorigo³⁹, A. Dosil Suárez³⁷, D. Dossett⁴⁸, A. Dovbnya⁴³, K. Dreimanis⁵², G. Dujany⁵⁴, F. Dupertuis³⁹, P. Durante³⁸, R. Dzhelyadin³⁵, A. Dziurda²⁶, A. Dzyuba³⁰, S. Easo^{49,38}, U. Egede⁵³, V. Egorychev³¹, S. Eidelman³⁴, S. Eisenhardt⁵⁰, U. Eitschberger⁹, R. Ekelhof⁹, L. Eklund⁵¹, I. El Rifai⁵, Ch. Elsasser⁴⁰, S. Ely⁵⁹, S. Esen¹¹, H.-M. Evans⁴⁷, T. Evans⁵⁵, A. Falabella¹⁴, C. Färber¹¹, C. Farinelli⁴¹, N. Farley⁴⁵, S. Farry⁵², R. Fay⁵², D. Ferguson⁵⁰, V. Fernandez Albor³⁷, F. Ferreira Rodrigues¹, M. Ferro-Luzzi³⁸, S. Filippov³³, M. Fiore^{16,f}, M. Fiorini^{16,f}, M. Firlej²⁷, C. Fitzpatrick³⁹, T. Fiutowski²⁷, P. Fol⁵³, M. Fontana¹⁰, F. Fontanelli^{19,j}, R. Forty³⁸, O. Francisco², M. Frank³⁸, C. Frei³⁸, M. Frosini¹⁷, J. Fu^{21,38}, E. Furfaro^{24,l}, A. Gallas Torreira³⁷, D. Galli^{14,d}, S. Gallorini^{22,38}, S. Gambetta^{19,j}, M. Gandelman², P. Gandini⁵⁹, Y. Gao³, J. García Pardiñas³⁷, J. Garofoli⁵⁹, J. Garra Tico⁴⁷, L. Garrido³⁶, D. Gascon³⁶, C. Gaspar³⁸, U. Gastaldi¹⁶, R. Gauld⁵⁵, L. Gavardi⁹, G. Gazzoni⁵, A. Geraci^{21,v}, E. Gersabeck¹¹, M. Gersabeck⁵⁴, T. Gershon⁴⁸, Ph. Ghez⁴, A. Gianelle²², S. Gianì³⁹, V. Gibson⁴⁷, L. Giubega²⁹, V.V. Gligorov³⁸, C. Göbel⁶⁰, D. Golubkov³¹, A. Golutvin^{53,31,38}, A. Gomes^{1,a}, C. Gotti^{20,k}, M. Grabalosa Gándara⁵, R. Graciani Diaz³⁶, L.A. Granado Cardoso³⁸, E. Graugés³⁶, E. Graverini⁴⁰, G. Graziani¹⁷, A. Grecu²⁹, E. Greening⁵⁵, S. Gregson⁴⁷, P. Griffith⁴⁵, L. Grillo¹¹, O. Grünberg⁶³, B. Gui⁵⁹, E. Gushchin³³, Yu. Guz^{35,38}, T. Gys³⁸, C. Hadjivasiliou⁵⁹, G. Haefeli³⁹, C. Haen³⁸, S.C. Haines⁴⁷, S. Hall⁵³,

B. Hamilton⁵⁸, T. Hampson⁴⁶, X. Han¹¹, S. Hansmann-Menzemer¹¹, N. Harnew⁵⁵,
 S.T. Harnew⁴⁶, J. Harrison⁵⁴, J. He³⁸, T. Head³⁹, V. Heijne⁴¹, K. Hennessy⁵², P. Henrard⁵,
 L. Henry⁸, J.A. Hernando Morata³⁷, E. van Herwijnen³⁸, M. Heß⁶³, A. Hicheur², D. Hill⁵⁵,
 M. Hoballah⁵, C. Hombach⁵⁴, W. Hulsbergen⁴¹, N. Hussain⁵⁵, D. Hutchcroft⁵², D. Hynds⁵¹,
 M. Idzik²⁷, P. Ilten⁵⁶, R. Jacobsson³⁸, A. Jaeger¹¹, J. Jalocha⁵⁵, E. Jans⁴¹, A. Jawahery⁵⁸,
 F. Jing³, M. John⁵⁵, D. Johnson³⁸, C.R. Jones⁴⁷, C. Joram³⁸, B. Jost³⁸, N. Jurik⁵⁹,
 S. Kandybei⁴³, W. Kanso⁶, M. Karacson³⁸, T.M. Karbach³⁸, S. Karodia⁵¹, M. Kelsey⁵⁹,
 I.R. Kenyon⁴⁵, T. Ketel⁴², B. Khanji^{20,38,k}, C. Khurewathanakul³⁹, S. Klaver⁵⁴,
 K. Klimaszewski²⁸, O. Kochebina⁷, M. Kolpin¹¹, I. Komarov³⁹, R.F. Koopman⁴²,
 P. Koppenburg^{41,38}, M. Korolev³², L. Kravchuk³³, K. Kreplin¹¹, M. Kreps⁴⁸, G. Krocker¹¹,
 P. Krokovny³⁴, F. Kruse⁹, W. Kucewicz^{26,o}, M. Kucharczyk^{20,26,k}, V. Kudryavtsev³⁴,
 K. Kurek²⁸, T. Kvaratskheliya³¹, V.N. La Thi³⁹, D. Lacarrere³⁸, G. Lafferty⁵⁴, A. Lai¹⁵,
 D. Lambert⁵⁰, R.W. Lambert⁴², G. Lanfranchi¹⁸, C. Langenbruch⁴⁸, B. Langhans³⁸,
 T. Latham⁴⁸, C. Lazzeroni⁴⁵, R. Le Gac⁶, J. van Leerdam⁴¹, J.-P. Lees⁴, R. Lefèvre⁵, A. Leflat³²,
 J. Lefrançois⁷, O. Leroy⁶, T. Lesiak²⁶, B. Leverington¹¹, Y. Li⁷, T. Likhomanenko⁶⁴, M. Liles⁵²,
 R. Lindner³⁸, C. Linn³⁸, F. Lionetto⁴⁰, B. Liu¹⁵, S. Lohn³⁸, I. Longstaff⁵¹, J.H. Lopes²,
 P. Lowdon⁴⁰, D. Lucchesi^{22,r}, H. Luo⁵⁰, A. Lupato²², E. Luppi^{16,f}, O. Lupton⁵⁵, F. Machefert⁷,
 I.V. Machikhiliyan³¹, F. Maciuc²⁹, O. Maev³⁰, S. Malde⁵⁵, A. Malinin⁶⁴, G. Manca^{15,e},
 G. Mancinelli⁶, A. Mapelli³⁸, J. Maratas⁵, J.F. Marchand⁴, U. Marconi¹⁴, C. Marin Benito³⁶,
 P. Marino^{23,t}, R. Märki³⁹, J. Marks¹¹, G. Martellotti²⁵, M. Martinelli³⁹, D. Martinez Santos⁴²,
 F. Martinez Vidal⁶⁵, D. Martins Tostes², A. Massafferri¹, R. Matev³⁸, Z. Mathe³⁸,
 C. Matteuzzi²⁰, A. Mazurov⁴⁵, M. McCann⁵³, J. McCarthy⁴⁵, A. McNab⁵⁴, R. McNulty¹²,
 B. McSkelly⁵², B. Meadows⁵⁷, F. Meier⁹, M. Meissner¹¹, M. Merk⁴¹, D.A. Milanes⁶²,
 M.-N. Minard⁴, N. Moggi¹⁴, J. Molina Rodriguez⁶⁰, S. Montei⁵, M. Morandin²², P. Morawski²⁷,
 A. Mordà⁶, M.J. Morello^{23,t}, J. Moron²⁷, A.-B. Morris⁵⁰, R. Mountain⁵⁹, F. Muheim⁵⁰,
 K. Müller⁴⁰, M. Mussini¹⁴, B. Muster³⁹, P. Naik⁴⁶, T. Nakada³⁹, R. Nandakumar⁴⁹, I. Nasteva²,
 M. Needham⁵⁰, N. Neri²¹, S. Neubert³⁸, N. Neufeld³⁸, M. Neuner¹¹, A.D. Nguyen³⁹,
 T.D. Nguyen³⁹, C. Nguyen-Mau^{39,q}, M. Nicol⁷, V. Niess⁵, R. Niet⁹, N. Nikitin³², T. Nikodem¹¹,
 A. Novoselov³⁵, D.P. O'Hanlon⁴⁸, A. Oblakowska-Mucha²⁷, V. Obraztsov³⁵, S. Ogilvy⁵¹,
 O. Okhrienko⁴⁴, R. Oldeman^{15,e}, C.J.G. Onderwater⁶⁶, M. Orlandea²⁹, B. Osorio Rodrigues¹,
 J.M. Otalora Goicochea², A. Otto³⁸, P. Owen⁵³, A. Oyanguren⁶⁵, B.K. Pal⁵⁹, A. Palano^{13,c},
 F. Palombo^{21,u}, M. Palutan¹⁸, J. Panman³⁸, A. Papanestis^{49,38}, M. Pappagallo⁵¹,
 L.L. Pappalardo^{16,f}, C. Parkes⁵⁴, C.J. Parkinson^{9,45}, G. Passaleva¹⁷, G.D. Patel⁵², M. Patel⁵³,
 C. Patrignani^{19,j}, A. Pearce^{54,49}, A. Pellegrino⁴¹, G. Penso^{25,m}, M. Pepe Altarelli³⁸,
 S. Perazzini^{14,d}, P. Perret⁵, L. Pescatore⁴⁵, E. Pesen⁶⁷, K. Petridis⁵³, A. Petrolini^{19,j},
 E. Picatoste Olloqui³⁶, B. Pietrzyk⁴, T. Pilar⁴⁸, D. Pinci²⁵, A. Pistone¹⁹, S. Playfer⁵⁰,
 M. Plo Casasus³⁷, F. Polci⁸, A. Poluektov^{48,34}, I. Polyakov³¹, E. Polycarpo², A. Popov³⁵,
 D. Popov¹⁰, B. Popovici²⁹, C. Potterat², E. Price⁴⁶, J.D. Price⁵², J. Prisciandaro³⁹,
 A. Pritchard⁵², C. Prouve⁴⁶, V. Pugatch⁴⁴, A. Puig Navarro³⁹, G. Punzi^{23,s}, W. Qian⁴,
 R. Quagliani^{7,46}, B. Rachwal²⁶, J.H. Rademacker⁴⁶, B. Rakotomiarana³⁹, M. Rama²³,
 M.S. Rangel², I. Raniuk⁴³, N. Rauschmayr³⁸, G. Raven⁴², F. Redi⁵³, S. Reichert⁵⁴, M.M. Reid⁴⁸,
 A.C. dos Reis¹, S. Ricciardi⁴⁹, S. Richards⁴⁶, M. Rihl³⁸, K. Rinnert⁵², V. Rives Molina³⁶,
 P. Robbe⁷, A.B. Rodrigues¹, E. Rodrigues⁵⁴, P. Rodriguez Perez⁵⁴, S. Roiser³⁸,
 V. Romanovsky³⁵, A. Romero Vidal³⁷, M. Rotondo²², J. Rouvinet³⁹, T. Ruf³⁸, H. Ruiz³⁶,
 P. Ruiz Valls⁶⁵, J.J. Saborido Silva³⁷, N. Sagidova³⁰, P. Sail⁵¹, B. Saitta^{15,e},
 V. Salustino Guimaraes², C. Sanchez Mayordomo⁶⁵, B. Sanmartin Sedes³⁷, R. Santacesaria²⁵,

C. Santamarina Rios³⁷, E. Santovetti^{24,l}, A. Sarti^{18,m}, C. Satriano^{25,n}, A. Satta²⁴, D.M. Saunders⁴⁶, D. Savrina^{31,32}, M. Schiller³⁸, H. Schindler³⁸, M. Schlupp⁹, M. Schmelling¹⁰, B. Schmidt³⁸, O. Schneider³⁹, A. Schopper³⁸, M.-H. Schune⁷, R. Schwemmer³⁸, B. Sciascia¹⁸, A. Sciubba^{25,m}, A. Semennikov³¹, I. Sepp⁵³, N. Serra⁴⁰, J. Serrano⁶, L. Sestini²², P. Seyfert¹¹, M. Shapkin³⁵, I. Shapoval^{16,43,f}, Y. Shcheglov³⁰, T. Shears⁵², L. Shekhtman³⁴, V. Shevchenko⁶⁴, A. Shires⁹, R. Silva Coutinho⁴⁸, G. Simi²², M. Sirendi⁴⁷, N. Skidmore⁴⁶, I. Skillicorn⁵¹, T. Skwarnicki⁵⁹, N.A. Smith⁵², E. Smith^{55,49}, E. Smith⁵³, J. Smith⁴⁷, M. Smith⁵⁴, H. Snoek⁴¹, M.D. Sokoloff⁵⁷, F.J.P. Soler⁵¹, F. Soomro³⁹, D. Souza⁴⁶, B. Souza De Paula², B. Spaan⁹, P. Spradlin⁵¹, S. Sridharan³⁸, F. Stagni³⁸, M. Stahl¹¹, S. Stahl¹¹, O. Steinkamp⁴⁰, O. Stenyakin³⁵, F. Sterpka⁵⁹, S. Stevenson⁵⁵, S. Stoica²⁹, S. Stone⁵⁹, B. Storaci⁴⁰, S. Stracka^{23,t}, M. Straticiuc²⁹, U. Straumann⁴⁰, R. Stroili²², L. Sun⁵⁷, W. Sutcliffe⁵³, K. Swientek²⁷, S. Swientek⁹, V. Syropoulos⁴², M. Szczekowski²⁸, P. Szczypka^{39,38}, T. Szumlak²⁷, S. T'Jampens⁴, M. Teklishyn⁷, G. Tellarini^{16,f}, F. Teubert³⁸, C. Thomas⁵⁵, E. Thomas³⁸, J. van Tilburg⁴¹, V. Tisserand⁴, M. Tobin³⁹, J. Todd⁵⁷, S. Tolk⁴², L. Tomassetti^{16,f}, D. Tonelli³⁸, S. Topp-Joergensen⁵⁵, N. Torr⁵⁵, E. Tournefier⁴, S. Tourneur³⁹, M.T. Tran³⁹, M. Tresch⁴⁰, A. Trisovic³⁸, A. Tsaregorodtsev⁶, P. Tsopelas⁴¹, N. Tuning⁴¹, M. Ubeda Garcia³⁸, A. Ukleja²⁸, A. Ustyuzhanin⁶⁴, U. Uwer¹¹, C. Vacca¹⁵, V. Vagnoni¹⁴, G. Valenti¹⁴, A. Vallier⁷, R. Vazquez Gomez¹⁸, P. Vazquez Regueiro³⁷, C. Vázquez Sierra³⁷, S. Vecchi¹⁶, J.J. Velthuis⁴⁶, M. Veltri^{17,h}, G. Veneziano³⁹, M. Vesterinen¹¹, JVVB Viana Barbosa³⁸, B. Viaud⁷, D. Vieira², M. Vieites Diaz³⁷, X. Vilasis-Cardona^{36,p}, A. Vollhardt⁴⁰, D. Volyansky¹⁰, D. Voong⁴⁶, A. Vorobyev³⁰, V. Vorobyev³⁴, C. Voß⁶³, J.A. de Vries⁴¹, R. Waldi⁶³, C. Wallace⁴⁸, R. Wallace¹², J. Walsh²³, S. Wandernoth¹¹, J. Wang⁵⁹, D.R. Ward⁴⁷, N.K. Watson⁴⁵, D. Websdale⁵³, M. Whitehead⁴⁸, D. Wiedner¹¹, G. Wilkinson^{55,38}, M. Wilkinson⁵⁹, M.P. Williams⁴⁵, M. Williams⁵⁶, H.W. Wilschut⁶⁶, F.F. Wilson⁴⁹, J. Wimberley⁵⁸, J. Wishahi⁹, W. Wislicki²⁸, M. Witek²⁶, G. Wormser⁷, S.A. Wotton⁴⁷, S. Wright⁴⁷, K. Wyllie³⁸, Y. Xie⁶¹, Z. Xing⁵⁹, Z. Xu³⁹, Z. Yang³, X. Yuan³, O. Yushchenko³⁵, M. Zangoli¹⁴, M. Zavertyaev^{10,b}, L. Zhang³, W.C. Zhang¹², Y. Zhang³, A. Zhelezov¹¹, A. Zhokhov³¹, L. Zhong³.

¹Centro Brasileiro de Pesquisas Físicas (CBPF), Rio de Janeiro, Brazil

²Universidade Federal do Rio de Janeiro (UFRJ), Rio de Janeiro, Brazil

³Center for High Energy Physics, Tsinghua University, Beijing, China

⁴LAPP, Université de Savoie, CNRS/IN2P3, Annecy-Le-Vieux, France

⁵Clermont Université, Université Blaise Pascal, CNRS/IN2P3, LPC, Clermont-Ferrand, France

⁶CPPM, Aix-Marseille Université, CNRS/IN2P3, Marseille, France

⁷LAL, Université Paris-Sud, CNRS/IN2P3, Orsay, France

⁸LPNHE, Université Pierre et Marie Curie, Université Paris Diderot, CNRS/IN2P3, Paris, France

⁹Fakultät Physik, Technische Universität Dortmund, Dortmund, Germany

¹⁰Max-Planck-Institut für Kernphysik (MPIK), Heidelberg, Germany

¹¹Physikalisches Institut, Ruprecht-Karls-Universität Heidelberg, Heidelberg, Germany

¹²School of Physics, University College Dublin, Dublin, Ireland

¹³Sezione INFN di Bari, Bari, Italy

¹⁴Sezione INFN di Bologna, Bologna, Italy

¹⁵Sezione INFN di Cagliari, Cagliari, Italy

¹⁶Sezione INFN di Ferrara, Ferrara, Italy

¹⁷Sezione INFN di Firenze, Firenze, Italy

¹⁸Laboratori Nazionali dell'INFN di Frascati, Frascati, Italy

¹⁹Sezione INFN di Genova, Genova, Italy

²⁰Sezione INFN di Milano Bicocca, Milano, Italy

²¹Sezione INFN di Milano, Milano, Italy

- ²²Sezione INFN di Padova, Padova, Italy
²³Sezione INFN di Pisa, Pisa, Italy
²⁴Sezione INFN di Roma Tor Vergata, Roma, Italy
²⁵Sezione INFN di Roma La Sapienza, Roma, Italy
²⁶Henryk Niewodniczanski Institute of Nuclear Physics Polish Academy of Sciences, Kraków, Poland
²⁷AGH - University of Science and Technology, Faculty of Physics and Applied Computer Science, Kraków, Poland
²⁸National Center for Nuclear Research (NCBJ), Warsaw, Poland
²⁹Horia Hulubei National Institute of Physics and Nuclear Engineering, Bucharest-Magurele, Romania
³⁰Petersburg Nuclear Physics Institute (PNPI), Gatchina, Russia
³¹Institute of Theoretical and Experimental Physics (ITEP), Moscow, Russia
³²Institute of Nuclear Physics, Moscow State University (SINP MSU), Moscow, Russia
³³Institute for Nuclear Research of the Russian Academy of Sciences (INR RAN), Moscow, Russia
³⁴Budker Institute of Nuclear Physics (SB RAS) and Novosibirsk State University, Novosibirsk, Russia
³⁵Institute for High Energy Physics (IHEP), Protvino, Russia
³⁶Universitat de Barcelona, Barcelona, Spain
³⁷Universidad de Santiago de Compostela, Santiago de Compostela, Spain
³⁸European Organization for Nuclear Research (CERN), Geneva, Switzerland
³⁹Ecole Polytechnique Fédérale de Lausanne (EPFL), Lausanne, Switzerland
⁴⁰Physik-Institut, Universität Zürich, Zürich, Switzerland
⁴¹Nikhef National Institute for Subatomic Physics, Amsterdam, The Netherlands
⁴²Nikhef National Institute for Subatomic Physics and VU University Amsterdam, Amsterdam, The Netherlands
⁴³NSC Kharkiv Institute of Physics and Technology (NSC KIPT), Kharkiv, Ukraine
⁴⁴Institute for Nuclear Research of the National Academy of Sciences (KINR), Kyiv, Ukraine
⁴⁵University of Birmingham, Birmingham, United Kingdom
⁴⁶H.H. Wills Physics Laboratory, University of Bristol, Bristol, United Kingdom
⁴⁷Cavendish Laboratory, University of Cambridge, Cambridge, United Kingdom
⁴⁸Department of Physics, University of Warwick, Coventry, United Kingdom
⁴⁹STFC Rutherford Appleton Laboratory, Didcot, United Kingdom
⁵⁰School of Physics and Astronomy, University of Edinburgh, Edinburgh, United Kingdom
⁵¹School of Physics and Astronomy, University of Glasgow, Glasgow, United Kingdom
⁵²Oliver Lodge Laboratory, University of Liverpool, Liverpool, United Kingdom
⁵³Imperial College London, London, United Kingdom
⁵⁴School of Physics and Astronomy, University of Manchester, Manchester, United Kingdom
⁵⁵Department of Physics, University of Oxford, Oxford, United Kingdom
⁵⁶Massachusetts Institute of Technology, Cambridge, MA, United States
⁵⁷University of Cincinnati, Cincinnati, OH, United States
⁵⁸University of Maryland, College Park, MD, United States
⁵⁹Syracuse University, Syracuse, NY, United States
⁶⁰Pontifícia Universidade Católica do Rio de Janeiro (PUC-Rio), Rio de Janeiro, Brazil, associated to ²
⁶¹Institute of Particle Physics, Central China Normal University, Wuhan, Hubei, China, associated to ³
⁶²Departamento de Fisica , Universidad Nacional de Colombia, Bogota, Colombia, associated to ⁸
⁶³Institut für Physik, Universität Rostock, Rostock, Germany, associated to ¹¹
⁶⁴National Research Centre Kurchatov Institute, Moscow, Russia, associated to ³¹
⁶⁵Instituto de Fisica Corpuscular (IFIC), Universitat de Valencia-CSIC, Valencia, Spain, associated to ³⁶
⁶⁶Van Swinderen Institute, University of Groningen, Groningen, The Netherlands, associated to ⁴¹
⁶⁷Celal Bayar University, Manisa, Turkey, associated to ³⁸

^aUniversidade Federal do Triângulo Mineiro (UFTM), Uberaba-MG, Brazil

^bP.N. Lebedev Physical Institute, Russian Academy of Science (LPI RAS), Moscow, Russia

^cUniversità di Bari, Bari, Italy

- ^d Università di Bologna, Bologna, Italy
^e Università di Cagliari, Cagliari, Italy
^f Università di Ferrara, Ferrara, Italy
^g Università di Firenze, Firenze, Italy
^h Università di Urbino, Urbino, Italy
ⁱ Università di Modena e Reggio Emilia, Modena, Italy
^j Università di Genova, Genova, Italy
^k Università di Milano Bicocca, Milano, Italy
^l Università di Roma Tor Vergata, Roma, Italy
^m Università di Roma La Sapienza, Roma, Italy
ⁿ Università della Basilicata, Potenza, Italy
^o AGH - University of Science and Technology, Faculty of Computer Science, Electronics and Telecommunications, Kraków, Poland
^p LIFAEELS, La Salle, Universitat Ramon Llull, Barcelona, Spain
^q Hanoi University of Science, Hanoi, Viet Nam
^r Università di Padova, Padova, Italy
^s Università di Pisa, Pisa, Italy
^t Scuola Normale Superiore, Pisa, Italy
^u Università degli Studi di Milano, Milano, Italy
^v Politecnico di Milano, Milano, Italy